Neuroscience Research xxx (2018) xxx–xxx

Contents lists available at ScienceDirect

Neuroscience Research

journal homepage: www.elsevier.com/locate/neures

Technical note

Monitoring brain neuronal activity with manipulation of cardiac events in a freely moving rat

Yu Shikano [a], Yuji Ikegaya [a,b], Takuya Sasaki [a,c,*]

[a] Graduate School of Pharmaceutical Sciences, The University of Tokyo, 7-3-1 Hongo Bunkyo-ku, Tokyo, 113-0033, Japan
[b] Center for Information and Neural Networks, Suita City, Osaka, 565-0871, Japan
[c] Precursory Research for Embryonic Science and Technology (PRESTO), Japan Science and Technology Agency (JST), 4-1-8 Honcho, Kawaguchi, Saitama 332-0012, Japan

ARTICLE INFO

Article history:
Received 18 December 2017
Received in revised form 9 February 2018
Accepted 13 February 2018
Available online xxx

Keywords:
Cardiac muscle stimulation
Vagus nerve stimulation
Electroencephalogram
Local field potential

ABSTRACT

Behavioral and cognitive studies have demonstrated that brain functions are affected by the activity states of the peripheral organs, such as the cardiac and respiratory systems. However, detailed neurophysiological mechanisms underlying the body-brain interactions remain unknown. In this study, we developed a method for manipulating activity levels of the heart using direct cardiac stimulation and vagus nerve stimulation that can be combined with recording cerebral local field potentials using a microdrive system, electrocardiograms, electromyograms, in a freely moving rat. With this method, the electrical stimulation to the heart increases heart rates up to 14 Hz, whereas the vagus nerve stimulation decreases heart rates to 3 Hz. Transient electrical artifacts arising from the peripheral stimulation are not contaminated in cortical local field potential signals low-pass filtered at 150 Hz and distinguishable from extracellular multiunit signals. The technique will contribute to understanding the neurophysiological correlate of mind-body associations in health and disease.

1. Introduction

The brain continuously monitors internal physiological states of the body, a process called interoception (Garfinkel and Critchley, 2016; Pfeifer et al., 2017). One example of interoception occurs when extracellular field potentials of the brain are affected by changes in electroencephalography signals of human subjects, which can be represented as heartbeat-evoked potentials (Fukushima et al., 2011; Kern et al., 2013). Furthermore, it has been shown that the amplitudes of heartbeat-evoked potentials are linked with task performance during a visual detection task (Park et al., 2014), and sensitivity in response to fearful events is enhanced during the systole phase of the heartbeat (Azevedo et al., 2017a,b; Garfinkel et al., 2014; Garfinkel and Critchley, 2016). Evidence therefore suggests that heartbeat signals influence brain activity and cognitive functions.

One pathway responsible for heart-brain signal transmission is the afferent vagus nerve (Garfinkel and Critchley, 2016). A number of clinical studies have shown that vagus nerve stimulation (VNS) is effective as a medical therapy for several central nervous system diseases in humans, such as epileptic seizures (Ben-Menachem et al., 1994; Takaya et al., 1996) and treatment-resistant depression (Nemeroff et al., 2006; Wani et al., 2013). Behavioral studies using rodents have demonstrated that VNS can stop seizures (Woodbury and Woodbury, 1990) and alter learning and emotional responses (Alvarez-Dieppa et al., 2016; Pena et al., 2014). The available evidence demonstrates that cardiac signals transmitted via the afferent vagus nerve also have a pronounced impact on brain information processing.

While the evidence for interoception at the behavioral level has been integrated, detailed neurophysiological mechanisms underlying body-brain signal interactions remain unclear. To address this issue, several pioneering studies have utilized experimental tools that can apply VNS to rodents while monitoring brain local field potentials (LFPs) with single or microarray electrodes (Alexander et al., 2017; Cao et al., 2016; Larsen et al., 2016; Usami et al., 2013). The limitation of these techniques was that it was difficult to detect neuronal spikes (so-called unit signals) from sufficient numbers of cells, ranging from tens to hundreds of cells, especially where the targeted cell population is restricted in a small space, such as the hippocampal cell layer, as the depth of individual electrodes was not adjustable once the electrodes were implanted into the tissue.

* Corresponding author at: Graduate School of Pharmaceutical Sciences, The University of Tokyo, 7-3-1 Hongo Bunkyo-ku, Tokyo, 113-0033, Japan.
E-mail address: tsasaki@mol.f.u-tokyo.ac.jp (T. Sasaki).

https://doi.org/10.1016/j.neures.2018.02.004
0168-0102/

For large-scale recordings of neuronal spike patterns in the brain, a microdrive system has been widely utilized that accommodates tens of tetrodes and enables to adjust the depth of individual electrodes after implantation (Buzsáki, 2004; Jog et al., 2002; Kloosterman et al., 2009; Nguyen et al., 2009). This system is applicable to recordings from multiple brain regions as the coordinates of electrodes are flexibly customized. The technical difficulty of a microdrive, however, is that it cannot be easily combined with a peripheral recording/manipulation due to the largeness of a microdrive with a diameter of approximately 4.5 cm and 3.0 cm and a weight of up to 25 g and 4 g for rats and mice, respectively.

We have recently established an *in vivo* electrophysiological recording method to capture LFPs from multiple brain regions along with electroencephalogram (ECG) and electromyogram (EMG) recordings in a freely moving rodent (Okada et al., 2016; Sasaki et al., 2017), termed the integrative microdrive system. In this study, we further extended this system by including stimulation electrodes for applying peripheral stimulation. This technique enables us to record brain LFP signals including spiking activity of multiple neurons, ECG, and EMG together and apply cardiac muscle stimulation (CMS) or a conventional VNS system to the same animals in real time. This paper describes procedures for the implantation of simulating and recording electrodes, and presents representative recording data showing how recorded electrical signals are affected by CMS and VNS.

2. Materials and methods

2.1. Animals

All experiments were performed with the approval of the animal experimental ethics committee at the University of Tokyo (approval number: P29-7) and in accordance with the NIH guidelines for the care and use of animals. A total of five Sprague-Dawley rats were purchased from SLC (Shizuoka, Japan). The animals were two to six months old, weighed 324–400 g, were maintained with free access to water and food, and were maintained under inverted 12-h light/12-h dark conditions (light from 8 pm to 8 am).

2.2. Preparation of the micro-drive array

An electrode assembly including recording electrodes, termed a micro-drive array, was prepared as described previously (Okada et al., 2016; Sasaki et al., 2017). Briefly, a micro-drive was composed of an electrical interface board (EIB) (EIB-36-PTB, Neuralynx, Inc., Bozeman, MT), an outer cover and a core body, which were custom-made by 3-D printers (UP Plus2, Tiertime, Beijing, China; MiniCraft, Young Optics, Hsinchu, Taiwan). An EIB had a sequence of metal holes (channels) for connections with wire electrodes, including 16–24 LFP channels, 1–2 ECG channels, 1–2 EMG channels, and 2 ground/reference (g/r) channels. The LFP channels were connected to tetrode wires, which are 17 μm polyimide-coated platinum-iridium (90/10%) wires (California Fine Wire Co., Grover Beach, CA) with an impedance adjusted to 150–300 kΩ. The ECG, EMG, and ground/reference channels were connected to insulated wires (~5 cm). The other ends of these wires were soldered to ECG, EMG, and ground/reference electrodes at surgery.

For the preparation of CMS electrodes, a bioflex wire (FEP Hookup Wire Stranded Stainless Steel AS 633, Cooner Wire Company, Chatsworth, CA) was cut into two 16-cm pieces, and the PTFE coating of the ends of these wire pieces was peeled off at lengths of ~5.0 mm on one end (short end) and ~10 mm on the other end (long end). A ring with a diameter of 0.6 mm at the long end was made by bending the wire, and the ring was fixed by soldering (Fig. 1A). A custom-made VNS electrode was created using a bioflex wire and a silicon tube (~7.0 mm), as described in a previous paper (Childs et al., 2015) (Fig. 1B).

2.3. Surgery

The animals were anesthetized with 3% isoflurane gas in O_2. They were then maintained with 1–2% isoflurane gas in air while lying on their backs. For each rat, either one of two surgeries were performed: (1) implantation of an electrode on the surface of the heart, termed the CMS method (Fig. 1A), or (2) implantation of electrodes on the vagus nerve, termed the VNS method (Fig. 1B). (1) For implanting an electrode on the heart, artificial ventilation using a ventilator (SN-480-7, Shinano, Tokyo, Japan) at a frequency of 50–60 breaths per minute was applied to the animals after insertion of a polyethylene tube (internal diameter, 2 mm; external diameter, 4 mm) into the mouth cavity. An incision was made in the right chest over the heart, and the pericardium was carefully removed with minimal damage. A CMS electrode was sutured in the vicinities of the sinus node and the apex (Fig. 1A). The chest cavity was closed. (2) For implanting an electrode on the vagus nerve, an incision was made in the left neck area, and the bundle including the vagus nerve and the carotid artery were isolated. A VNS electrode was attached to the vagus nerve (Fig. 1B). The muscle tube surrounding the trachea was closed, and the open ends of the electrodes were extruded from the incision.

After the electrode implantation at the peripheral sites, all rats underwent surgery to implant ECG, EMG, and LFP electrodes as described previously (Okada et al., 2016; Sasaki et al., 2017). Briefly, two ECG electrodes (stainless-steel wires; AS633, Cooner Wire Company) were attached to the intercostal muscles on both sides of the chest, and two EMG electrodes were sutured to the dorsal neck area. For implanting LFP electrodes on the hippocampus, a midline incision was made above the skull, and circular craniotomies 1.5 mm in diameter were made with a high speed drill (SD-102, Narishige, Tokyo, Japan) at coordinates of 4.0 mm posterior and 2.7 mm unilateral to bregma for the right hippocampus. The micro-drive array was placed above the craniotomy with tetrodes inserted ~1.25 mm into the brain tissue. Stainless-steel screws were implanted on the surface of the prefrontal cortex as ground/reference (g/r) electrodes. Finally, the open edges of the ECG electrodes, EMG electrodes, and g/r electrodes were soldered to the open edges of the insulated wires protruding from the corresponding channels on the EIB. All these wires and the micro-drive array were secured to the skull using dental cement. The open ends of the CMS/VNS electrodes were maintained protruding from the dental cement and were soldered to a socket attached to the micro-drive array (Fig. 1C). The socket was attached to the core of the micro-drive array. After fixing all the electrodes on the animals' heads, the animals were recovered from anesthesia. Over a period of approximately 1 week after surgery, the tetrodes were lowered approximately 100 μm per day to target brain regions, as determined by referencing individual LFP signals.

2.4. Stimulation of peripheral organs and electrophysiological recordings

For stimulating the peripheral organs, the socket was connected to an electrical stimulator (SEN-3301, Nihon Kohden, Tokyo, Japan). For recording electrophysiological signals, the EIB of the micro-drive array was connected to a digital headstage Cereplex M (Blackrock Microsystems, Salt Lake City, UT), and the digitized signals were transferred to a data acquisition system Cereplex Direct (Blackrock Microsystems). Electrical signals (LFPs, ECG, EMG) were recorded at a sampling rate of 2 kHz.

During recordings, animals were located in a recording box (25×30 cm^2) with a wall height of 50 cm. Trains of electrical pulses

Please cite this article in press as: Shikano, Y., et al., Monitoring brain neuronal activity with manipulation of cardiac events in a freely moving rat. Neurosci. Res. (2018), https://doi.org/10.1016/j.neures.2018.02.004

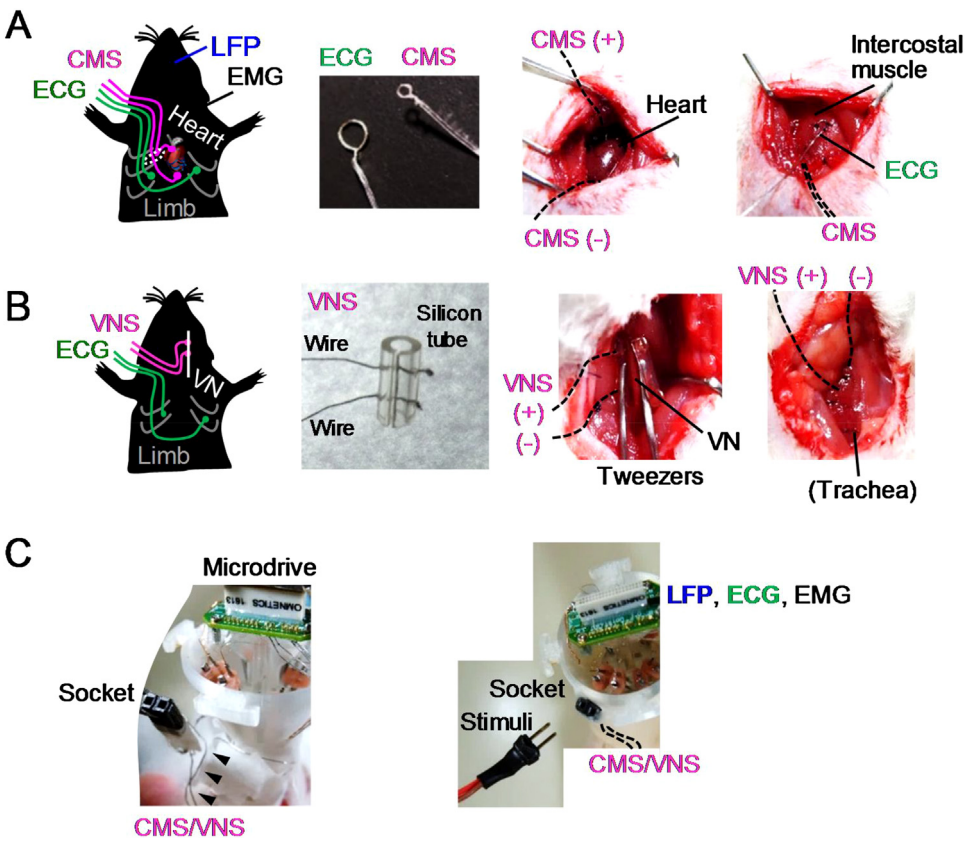

Fig. 1. Surgical procedures for implanting stimulation electrodes on the cardiac muscles and vagus nerves. (A) (From left to right) Schematic illustration showing how CMS electrodes (magenta) and ECG electrodes (green) are implanted. An image showing the tips of a CMS electrode and an ECG electrode. Two magnified images showing a CMS electrode and an ECG electrode sutured to the cardiac muscle and the intercostal muscles, respectively. Dashed lines indicate the electrode wires protruding from the tissue. (B) VNS electrode implantation, similar to panel A. An image showing the tip of a cuff-shaped VNS electrode that was created from a bioflex wire and a silicon tube. Two magnified images showing that the isolated vagus nerve was covered with the VNS electrode and the open ends of the VNS electrode were extruded from the incision after closing the muscle tube surrounding the trachea. (C) (left) At the final step of the surgery, the open ends of the CMS or VNS electrodes were soldered to wires from a socket that was attached to the core of a micro-drive array. (right) When recording, the socket was connected to a plug that transmitted electrical pulses for CMS and VNS.

with a pulse duration of 300 μs or 5 ms were applied to the peripheral organs (the heart or the vagus nerve, respectively) with a varying interval ranging from 50 to 500 ms and a varying amplitude ranging from 0 to 3.0 mA. An analog input system from the electric stimulator to the data acquisition system via BNC connectors specify the timings of electrical pulses during recording. LFP recordings were sampled at 2 kHz and low-pass filtered at 500 Hz. The unit activity was amplified and bandpass filtered at 250 Hz to 6 kHz. Spike waveforms above a trigger threshold (60 μV) were time-stamped and recorded at 30 kHz in a time window of 1.6 ms.

2.5. Histology of brain tissue

The rats were perfused intracardially with cold 4% paraformaldehyde in 25 mM phosphate-buffered saline and decapitated. The tetrodes were carefully removed from the brains. The brains were coronally sectioned at a thickness of 50 μm, and mounted on coverslips with PARA mount D (Falma, Tokyo, Japan).

2.6. Spike unit analysis

Spike sorting was performed offline using the graphical cluster-cutting software Mclust (Redish, 2009). Clustering was performed manually in 2D projections of the multidimensional parameter space (i.e., comparisons between the waveform amplitudes, waveform energies, and first principal component coefficient (PC1) of the energy normalized waveform, each measured on the four channels of each tetrode).

2.7. Data analysis

LFP traces were bandpass filtered at 1–250 Hz. ECG traces were bandpass filtered at 10–200 Hz, and beat-to-beat intervals (R-R interval) were calculated from the timestamp of the R-wave peak. EMG traces were high-pass filtered at 100 Hz. For the detection of hippocampal ripple events, hippocampal LFP traces were bandpass filtered at 150–250 Hz, and the root mean-square (RMS) power was calculated with a bin size of 5 ms. The threshold for awake-ripple detection was set to 3 standard deviation above the mean with a duration of more than 20 ms. To compute the time–frequency representation of LFP power, LFP signals were convolved by a complex Morlet wavelet transformation at a frequency ranging from 1 to 250 Hz. The absolute power spectrum of the LFP during each 0.5-ms time window was calculated, and z-scores were computed for each frequency band across an entire analyzed period.

All analyses were performed in Matlab (Mathworks).

3. Results

3.1. Cardiac stimulation with cortical LFP and ECG recordings

A CMS electrode was attached to the cardiac muscles of rats in addition to implantation of LFP, ECG, and EMG electrodes (Fig. 2A). The rats had baseline heart rates of 5–8 Hz, corresponding to 300–480 beats per minute (bpm) (Fig. 2B, top). In the rats, trains of electrical pulse of CMS (300 μs) were applied at a varying frequency ranging from 2 Hz to 20 Hz (Fig. 2B–D). The CMS current

Please cite this article in press as: Shikano, Y., et al., Monitoring brain neuronal activity with manipulation of cardiac events in a freely moving rat. Neurosci. Res. (2018), https://doi.org/10.1016/j.neures.2018.02.004

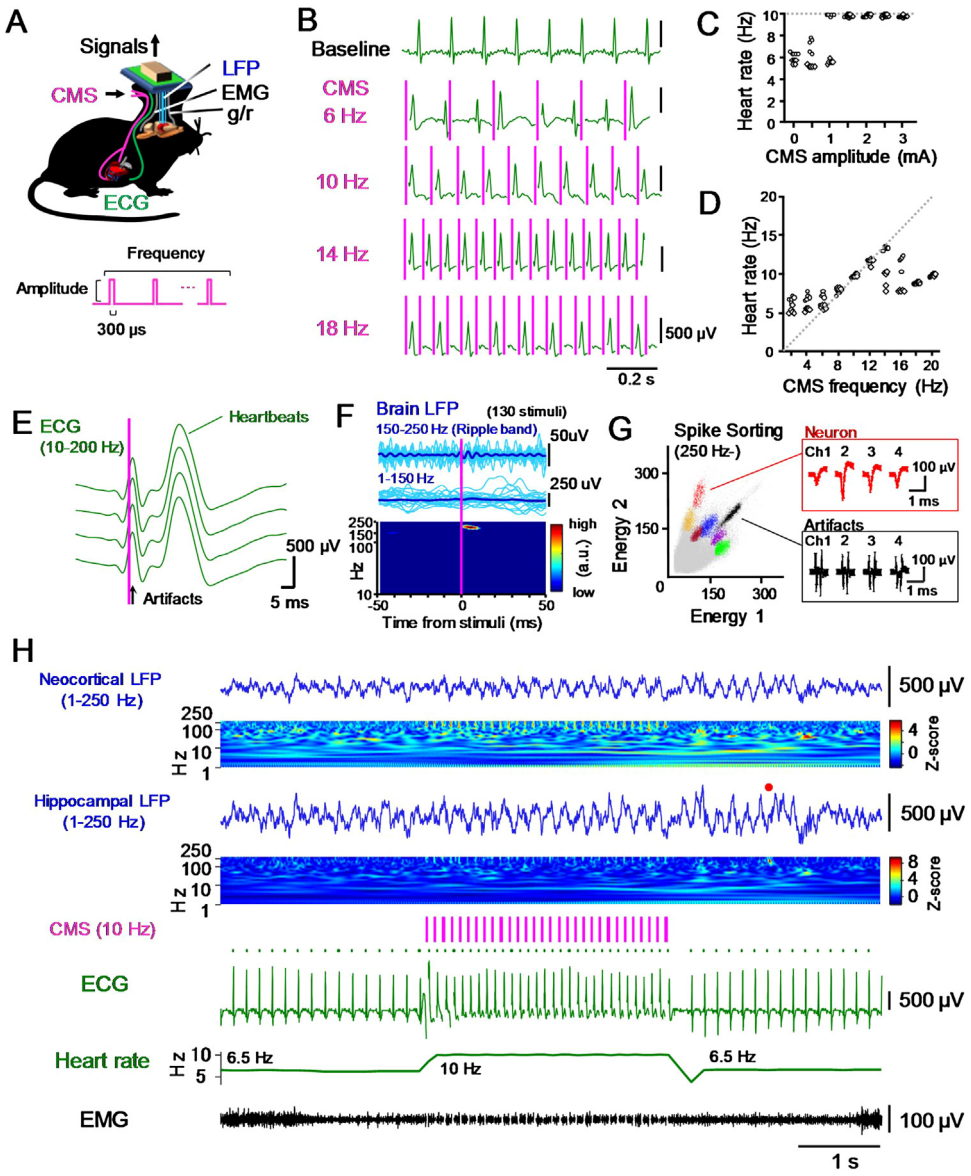

Fig. 2. Applying CMS during the recording of LFP and ECG signals. (A) Schematic illustration of the experimental configuration from a freely moving rat. (B) (From top to bottom) Representative ECG traces without CMS and in response to CMS at frequencies of 6, 10, 14 and 18 Hz. Each vertical magenta line indicates the timing of stimulation (1.5 mA, 300 μs). (C) The CMS at 10 Hz was applied with varying CMS amplitudes. CMS with an amplitude greater than 1.0 mA can induce heartbeats at a corresponding frequency, demonstrating that the threshold to induce a heartbeat is 1.0 mA. (D) Relationship between the frequency of the above-threshold CMS (x-axis) and the frequency of evoked heartbeats (y-axis). The gray diagonal line indicates where the evoked frequency is equal to the stimulus frequency. (E) Representative ECG traces including an electrical artifact derived from CMS and an evoked heartbeat. The vertical magenta line indicates the timing of a stimulus (2.5 mA, 300 μs). (F) (Top) Representative hippocampal LFP traces band-pass filtered at 150–250 Hz (ripple band) and 1–150 Hz during CMS. Each thin cyan line indicates a LFP trace aligned to stimulus timing from each trial and the thick blue line indicates an averaged trace. (Bottom) The power spectrum constructed from the averaged LFP trace. Note a stimulus-triggered change in LFP power at the ripple band while there are no apparent power changes at the lower bands. (G) Cluster plots showing the energy of multiunit signals recorded from two channels. Each dot represents a spike signal, and each color represents each cluster that was assigned to a single cell. The cluster shown in black represent CMS-induced electrical artifacts, demonstrating that clusters of real spikes and CMS-induced electrical artifacts are distinguishable. The insets represent average spike waveforms of a real cell and electrical artifacts. The artifact signal has two distinct peaks as it represents the onset and offset of CMS (300 μs). (H) (From top to bottom) Cortical LFP, hippocampal LFP signals, and the corresponding power spectrum constructed from the LFP signals, timing of CMS, ECG signal, EMG, the corresponding heart rates, and EMG signals. The red dot above the hippocampal LFP trace represents a ripple event. The green dots above the ECG trace indicate the timing of heartbeats. For clearer visualization, CMS-derived electrical artifacts included in ECG and EMG signals were truncated.

pulse generated an electrical artifact with a positive deflection of ~0.5 mV and ~10 ms in the ECG trace (Fig. 2E), which was distinguishable from individual R-peaks of heartbeats that typically had an amplitude of 0.5–1.0 mV and a duration of ~20 ms. In the CMS method, the threshold of the amplitude of an electrical pulse for inducing a heartbeat was determined in individual rats (Fig. 2C). The minimum current amplitude of CMS required for inducing a heartbeat was 1.0 mA, and the average latency between an above-threshold CMS pulse and the evoked heartbeat was 21.1 ± 1.7 ms.

When applying the above-threshold CMS pulses at a frequency of 8–12 Hz, the timing of heartbeats was perfectly synchronized to that of current pulses (Fig. 2D), demonstrating that cardiac pacing by CMS was successful at this frequency range. At a stimulus frequency of 14 Hz, 81.4% of electrical pulses of CMS successfully evoked stimulus-synchronized heartbeats. Stimuli at a frequency below 6 Hz or above 16 Hz failed to induce stimulus-synchronized heartbeats at the corresponding frequency (Fig. 2D).

Please cite this article in press as: Shikano, Y., et al., Monitoring brain neuronal activity with manipulation of cardiac events in a freely moving rat. Neurosci. Res. (2018), https://doi.org/10.1016/j.neures.2018.02.004

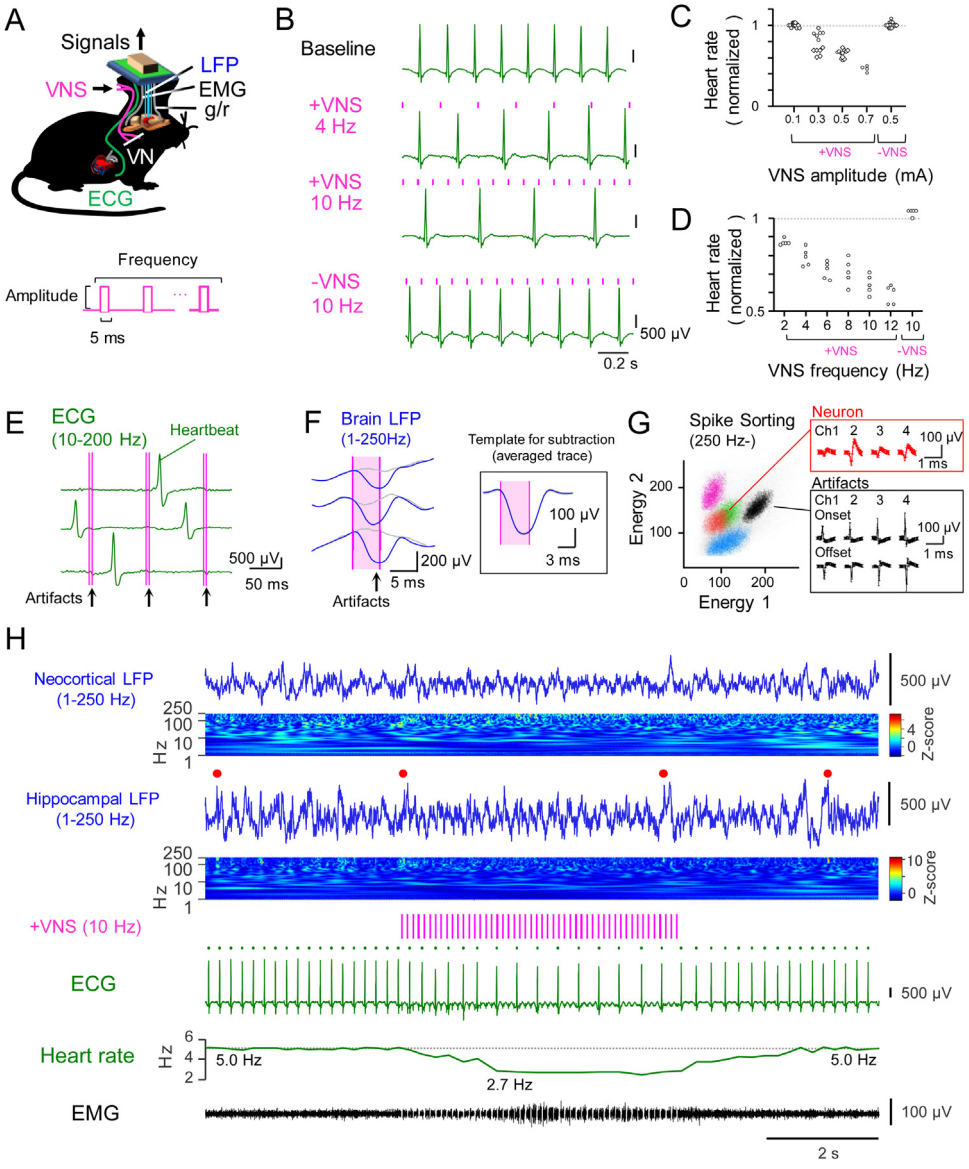

Fig. 3. Applying VNS during the recording of LFP and ECG signals. (A) Schematic illustration of the experimental configuration from a freely moving rat. (B) (From top to bottom) Representative ECG traces without VNS and in response to VNS with a direction from the cathode to the anode (termed +VNS) at a frequency of 4 and 10 Hz, as well as in the opposite direction (termed −VNS) at 10 Hz. The vertical magenta lines indicate the timing of stimulation (0.5 mA, 5 ms). (C) Normalized heart rates in response to +VNS at 10 Hz with varying amplitudes. The plot shows that the threshold of +VNS that reduces heartbeats is above 0.3 mA. (D) Relationship between the frequency of the above-threshold +VNS (x-axis) and the frequency of evoked heartbeats (y-axis). (E) Representative ECG traces in response to VNS. The vertical magenta lines indicate the timing of stimulation (0.5 mA, 5 ms). (F) Representative cortical LFP traces band-pass filtered at 1–150 Hz during VNS (original trace, blue; subtracted trace, gray). The right inset shows the VNS-triggered average of LPP trace, which was used as a template trace for subtraction of LFP signals. (G) Similar results as in Fig. 2G but plotted for +VNS. The onset and offset of VNS induced an upward and downward artifact unit signals, respectively. (H) Similar results as in Fig. 2H, but shown for +VNS at 10 Hz. The red dots above the hippocampal LFP trace represent ripple events. The horizontal dotted line indicates average heart rates before applying +VNS.

We evaluated whether brain LFP signals were contaminated with CMS-derived artifact electrical signals. CMS-triggered hippocampal LFP signals were filtered at a frequency band of 150–250 Hz and 1–150 Hz, a frequency band, including delta, theta, gamma bands (Fig. 2F). As shown in the averaged LFP traces (thick blue lines) and the corresponding power spectrum, LFP signals at a 150–250 Hz band included electrical artifacts derived from CMS, whereas no apparent CMS-induced artifacts were detected in LFP signals at a frequency band less than 150 Hz, demonstrating that the stimulus artifact was negligible for LFP power at a frequency below 150 Hz. As the frequency band of 150–250 Hz corresponds with a frequency band that is typically used for hippocampal ripple detection analysis, there is a concern that CMS-induced artifact may be detected as a ripple event. We excluded this possibility by showing that CMS-induced artifact waveforms were not detected by standard ripple detection criteria in which the root mean-square power of filtered signals continuously exceeded 3 standard deviation above the mean for a duration of at least 20 ms (see an example trace in Fig. 2H). This result was reasonable as the minimum duration for ripple detection is 20 ms, which is longer than CMS-induced artifacts with a duration of up to 10 ms. Next, we analyzed whether CMS-induced electrical artifacts were detected in LFP traces high-pass filtered at 250 Hz, a frequency band that is generally used for analysis of multiunit signals representing neuronal spikes (Fig. 2G). The waveforms of electrical artifacts were different from those of spike signals of individual neurons, which led to an apparently distinct cluster (the black cluster in Fig. 2G) formed by the artifacts in spike sorting planes compared with those

Please cite this article in press as: Shikano, Y., et al., Monitoring brain neuronal activity with manipulation of cardiac events in a freely moving rat. Neurosci. Res. (2018), https://doi.org/10.1016/j.neures.2018.02.004

of spikes of putative neurons (colored clusters). This result demonstrates that neuronal spike waveform is easily distinguishable from CMS-derived electrical artifacts. However, we need to note that, as the CMS-induced artifacts are originally detected by conventional multiunit recording systems that automatically extract LFP signals when the amplitude of signals exceed a certain threshold, we cannot correctly detect neuronal spikes that perfectly synchronized with CMS-induced artifacts within a duration of a spike window (in our case, 1.6 ms). Fig. 2H shows representative LFP and ECG traces during an application of CMS in a freely moving rat. While there appeared some changes in cortical LFP traces in response to CMS, indicating a peripheral-central transmission, we avoid further mentioning this biological phenomenon as the purpose of this paper is to specifically focus on methodological development.

3.2. Vagus nerve stimulation with cortical LFP and ECG recordings

For stimulating the vagus nerve, the anode and the cathode of VNS electrodes were attached; the anode was attached to periphery along the vagus nerve, and the cathode was attached to the brain side (Fig. 3A). Application of VNS from the anode to the cathode, termed +VNS, evoked pronounced decreases in heart rates (Fig. 3B). The minimal intensity of the +VNS to induce a heart rate change was 0.3 mA (Fig. 3C). The decrease in the heart rate strongly depended on the frequencies of +VNS pulses; above-threshold +VNS at a frequency of 4 Hz and 10 Hz decreased heart rates to 5.2 Hz (310 bpm) and 3.2 Hz (194 bpm), corresponding with 20% and 64% reductions compared to baseline heart rates, respectively (Fig. 3D). In contrast, VNS with the opposite direction, termed −VNS, failed to change heart rates (Fig. 3B–D). As in Fig. 2E, VNS-derived electrical artifacts had negative deflections and were distinguishable from heartbeat signals in ECG traces (Fig. 3E). Unlike CMS, VNS with a duration of 5 ms induced an electrical artifact with a negative deflection in cortical LFP traces low-pass filtered at 150 Hz (Fig. 3F, blue traces). The electrical artifacts were minimized (Fig. 3F, shown in grey) by subtracting a stimulus-triggered average LFP signal (Fig. 3F, inset), termed the template artifact trace, from the original LFP traces (Fig. 3F, blue traces). As in Fig. 2G, we also evaluated whether VNS interfered with multiunit signals (Fig. 3G). VNS-derived electrical artifacts were specifically detected at the onset and offset of VNS current pulses, as represented by two sets of four black waveforms (Fig. 3G, bottom box). The VNS-derived artifacts formed distinct clusters (black clusters) in the spike sorting planes, similar to the CMS-derived artifacts, and were dissociable from clusters of spike signals from real neurons (colored clusters). Fig. 3H shows representative LFP and ECG traces around VNS simultaneously obtained from a freely moving rat.

4. Discussion

In this study, we established a novel electrophysiological system that enabled us to perform electrical stimulations of the heart or the vagus nerve while performing brain multisite LFP recordings using a microdrive system in a freely moving rat. With our CMS method, perfect cardiac pacing was achieved at a frequency range of 8–12 Hz, corresponding to 480–720 bpm; the heart rate immediately returned to its baseline levels several seconds after stopping the stimulation, indicating the reversibility of cardiac rhythm stimulation. In our VNS method, heart rates were decreased to 4 Hz (240 bpm) depending on the frequency of stimulation. The limitations of this cardiac pacing within this frequency range are due to the inherent physiological properties of cardiac rhythms. We need to note that VNS may affect the other peripheral organs via nerve transmission. Further studies are required to evaluate effects of VNS in addition to heart rate changes.

Combining electrical stimulation of the peripheral organs with brain LFP recordings raises a concern that stimulus-induced electrical noise may extend into LFP signals. We showed that filtered LFP signals below 150 Hz were not contaminated with CMS-derived electrical artifacts. VNS-derived electrical artifacts with a duration of 5 ms were inevitably included in the filtered LFP traces, but these could be counteracted by subtracting a typical artifact waveform from the LFP traces. These results suggest that LFP analysis at frequency bands below 150 Hz, which typically include delta, theta, and gamma oscillations of neuronal populations, was not disrupted by CMS and VNS. Moreover, we showed that while both CMS and VNS-derived electrical artifacts were detected in LFP signals high-pass filtered at 250 Hz, they were easily distinguishable from true neuronal signals by spike-sorting analysis.

Compared with pharmacological tools, our technique using electrical stimulation has an advantage that allows us to manipulate peripheral organs at a temporal resolution on the scale of millisecond. Optogenetic stimulation of the heart is an alternative method for cardiac pacing that has been recently developed (Jia et al., 2011; Montgomery et al., 2016; Nussinovitch and Gepstein, 2015; Vogt et al., 2015; Weinberger et al., 2017). While the advantage of optogenetic manipulation is that it is completely free of electrical artifacts in electrophysiological signals, the optogenetic method requires both the injection of a large amount of virus (approximately 10^{13} viral genomes) (Nussinovitch and Gepstein, 2015) into the heart to generate sufficient expression of photosensitive proteins, such as channelrhodopsin 2, in cardiomyocytes and a photostimulation system to illuminate the heart.

To obtain stable electrical stimulation and recordings with a high signal-to-noise ratio, several training surgeries were required for an experimenter to become sufficiently skilled to complete all procedures, including thoracotomy, attachment of stimulation/recording electrodes, and soldering wires. The duration of thoracotomy surgery should be as short as possible under aseptic conditions, and the damage to the heart and vagus nerves should be minimized when the electrodes are attached to the tissue.

The methodological concept reported here will be applicable to many biological research issues concerning brain-body associations, and this system suggests detailed physiological mechanisms underlying the causal relationship between brain functions, including cognition and emotion, and signals from peripheral organs.

Conflicts of interest

The authors declare no conflicts of interest.

Acknowledgments

This work was supported by Kaken-hi (17H05939; 17H05551), a Grant in aid for Precursory Research for Embryonic Science and Technology from the Japan Science and Technology Agency, the Nakatomi Foundation, and the Suzuken Memorial Foundation.

References

Alexander, G.M., Huang, Y., Soderblom, E.J., He, X.P., Moseley, A.M., McNamara, J.O., 2017. Vagal nerve stimulation modifies neuronal activity and the proteome of excitatory synapses of amygdala/piriform cortex. J. Neurochem. 140, 629–644.
Alvarez-Dieppa, A.C., Griffin, K., Cavalier, S., McIntyre, C.K., 2016. Vagus nerve stimulation enhances extinction of conditioned fear in rats and modulates arc protein, CaMKII, and gluN2B-containing NMDA receptors in the basolateral amygdala. Neural Plast. 2016, 4273280.
Azevedo, R.T., Badoud, D., Tsakiris, M., 2017a. Afferent cardiac signals modulate attentional engagement to low spatial frequency fearful faces. Cortex, http://dx.doi.org/10.1016/j.cortex.2017.1006.1016.
Azevedo, R.T., Garfinkel, S.N., Critchley, H.D., Tsakiris, M., 2017b. Cardiac afferent activity modulates the expression of racial stereotypes. Nat. Comm. 8, 13854.
Ben-Menachem, E., Manon-Espaillat, R., Ristanovic, R., Wilder, B.J., Stefan, H., Mirza, W., Tarver, W.B., Wernicke, J.F., 1994. Vagus nerve stimulation for treatment of

partial seizures: 1. A controlled study of effect on seizures. First International Vagus Nerve Stimulation Study Group. Epilepsia 35, 616–626.
Buzsáki, G., 2004. Large-scale recording of neuronal ensembles. Nat. Neurosci, 7.
Cao, B., Wang, J., Shahed, M., Jelfs, B., Chan, R.H.M., Li, Y., 2016. Vagus nerve stimulation alters phase synchrony of the anterior cingulate cortex and facilitates decision making in rats. Sci. Rep. 6, 35135.
Childs, J.E., Alvarez-Dieppa, A.C., McIntyre, C.K., Kroener, S., 2015. Vagus nerve stimulation as a tool to induce plasticity in pathways relevant for extinction learning. J. Vis. Exp.: JoVE, e53032.
Fukushima, H., Terasawa, Y., Umeda, S., 2011. Association between interoception and empathy: evidence from heartbeat-evoked brain potential. Int. J. Psychophysiol. 79, 259–265.
Garfinkel, S.N., Critchley, H.D., 2016. Threat and the body: how the heart supports fear processing. Trends Cogn. Sci. 20, 34–46.
Garfinkel, S.N., Minati, L., Gray, M.A., Seth, A.K., Dolan, R.J., Critchley, H.D., 2014. Fear from the heart: sensitivity to fear stimuli depends on individual heartbeats. J. Neurosci. 34, 6573–6582.
Jia, Z., Valiunas, V., Lu, Z., Bien, H., Liu, H., Wang, H.-Z., Rosati, B., Brink, P.R., Cohen, I.S., Entcheva, E., 2011. Stimulating cardiac muscle by light cardiac optogenetics by cell delivery. Circulation: Arrhythmia Electrophysiol. 4, 753–760.
Jog, M.S., Connolly, C.I., Kubota, Y., Iyengar, D.R., Garrido, L., Harlan, R., Graybiel, A.M., 2002. Tetrode technology: advances in implantable hardware, neuroimaging, and data analysis techniques. J. Neurosci. Methods 117, 141–152.
Kern, M., Aertsen, A., Schulze-Bonhage, A., Ball, T., 2013. Heart cycle-related effects on event-related potentials, spectral power changes, and connectivity patterns in the human ECoG. Neuroimage 81, 178–190.
Kloosterman, F., Davidson, T.J., Gomperts, S.N., Layton, S.P., Hale, G., Nguyen, D.P., Wilson, M.A., 2009. Micro-drive array for chronic in vivo recording: drive fabrication. JoVE 1094.
Larsen, L., Wadman, W., van Mierlo, P., Delbeke, J., Grimonprez, A., Nieuwenhuyse, B., Portelli, J., Boon, P., Vonck, K., Raedt, R., 2016. Modulation of hippocampal activity by vagus nerve stimulation in freely moving rats. Brain Stimul. 9, 124–132.
Montgomery, K.L., Iyer, S.M., Christensen, A.J., Deisseroth, K., Delp, S.L., 2016. Beyond the brain: optogenetic control in the spinal cord and peripheral nervous system. Sci. Transl. Med. 8, 337rv335.
Nemeroff, C.B., Mayberg, H.S., Krahl, S.E., McNamara, J., Frazer, A., Henry, T.R., George, M.S., Charney, D.S., Brannan, S.K., 2006. VNS therapy in treatment-resistant depression: clinical evidence and putative neurobiological mechanisms. Neuropsychopharmacology 31, 1345–1355.
Nguyen, D.P., Layton, S.P., Hale, G., Gomperts, S.N., Davidson, T.J., Kloosterman, F., Wilson, M.A., 2009. Micro-drive array for chronic in vivo recording: tetrode assembly. JoVE 1098.
Nussinovitch, U., Gepstein, L., 2015. Optogenetics for in vivo cardiac pacing and resynchronization therapies. Nat. Biotechnol. 33, 750–754.
Okada, S., Igata, H., Sakaguchi, T., Sasaki, T., Ikegaya, Y., 2016. A new device for the simultaneous recording of cerebral, cardiac, and muscular electrical activity in freely moving rodents. J. Pharmacol. Sci. 132, 105–108.
Park, H.-D., Correia, S., Ducorps, A., Tallon-Baudry, C., 2014. Spontaneous fluctuations in neural responses to heartbeats predict visual detection. Nat. Neurosci. 17, 612–618.
Pena, D.F., Childs, J.E., Willett, S., Vital, A., McIntyre, C.K., Kroener, S., 2014. Vagus nerve stimulation enhances extinction of conditioned fear and modulates plasticity in the pathway from the ventromedial prefrontal cortex to the amygdala. Front. Behav. Neurosci. 8, 327.
Pfeifer, G., Garfinkel, S.N., van Praag, C.D., Sahota, K., Betka, S., Critchley, H.D., 2017. Feedback from the heart Emotional learning and memory is controlled by cardiac cycle, interoceptive accuracy and personality. Biol. Psychol. 126, 19–29.
Redish, A.D., 2009. MClust 3.5, Free-Ware Spike Sorting. University of Minnesota, Minneapolis, Available at http://redishlab.neuroscience.umn.edu/MClust/MClust.html.
Sasaki, T., Nishimura, Y., Ikegaya, Y., 2017. Simultaneous recordings of central and peripheral bioelectrical signals in a freely moving rodent. Biol. Pharm. Bull. 40, 711–715.
Takaya, M., Terry, W.J., Naritoku, D.K., 1996. Vagus nerve stimulation induces a sustained anticonvulsant effect. Epilepsia 37, 1111–1116.
Usami, K., Kano, R., Kawai, K., Noda, T., Ishiramatsu, T., Saito, N., Takahashi, H., 2013. Modulation of cortical synchrony by vagus nerve stimulation in adult rats. 2013. 35th Annual International Conference of the IEEE Engineering in Medicine and Biology Society (EMBC) 1, 5348–5351.
Vogt, C.C., Bruegmann, T., Malan, D., Ottersbach, A., Roell, W., Fleischmann, B.K., Sasse, P., 2015. Systemic gene transfer enables optogenetic pacing of mouse hearts. Cardiovasc. Res. 106, 338–343.
Wani, A., Trevino, K., Marnell, P., Husain, M.M., 2013. Advances in brain stimulation for depression. Ann. Clin. Psychiatry 25, 217–224.
Weinberger, F., Mannhardt, I., Eschenhagen, T., 2017. Engineering cardiac muscle tissue: a maturating field of research. Circ. Res. 120, 1487–1500.
Woodbury, D.M., Woodbury, J.W., 1990. Effects of vagal stimulation on experimentally induced seizures in rats. Epilepsia 31 (Suppl. 2), S7–19.

Please cite this article in press as: Shikano, Y., et al., Monitoring brain neuronal activity with manipulation of cardiac events in a freely moving rat. Neurosci. Res. (2018), https://doi.org/10.1016/j.neures.2018.02.004